

R.F. Banks \*, M.A. Bourassa, P. Hughes, J.J. O'Brien, and S.R. Smith

Center for Ocean-Atmospheric Prediction Studies (COAPS), The Florida State University, Tallahassee, Florida

## 1. INTRODUCTION

In 1997 the Indian summer monsoon triggered the wettest year on record in East Africa, sparking a deadly outbreak of mosquito-borne Rift Valley Fever and malaria in livestock and people. The 1997 monsoon event was associated with other ocean-atmospheric phenomenon. The two other phenomena that co-occurred in 1997-1998 were an El-Niño phase of the El-Niño Southern Oscillation (ENSO) and a positive phase of the Indian Ocean Dipole (IOD) mode. Through better understanding of the variability modulating the monsoon, predictions may be made sooner and millions of lives could be spared.

Surface fluxes of heat and momentum provide the link in the interaction between the atmosphere and the ocean (Jones et al. 1995). The need is there for providing high resolution, regularly gridded data for studying the variability of surface turbulent fluxes and for use in coupled ocean-atmosphere climate models. Therefore the purpose of our research is two-fold. The first goal is to use a new method of objectively gridding in-situ ship and buoy observations to provide an accurate representation of surface fluxes in the Indian Ocean. The second goal is to analyze spatial and temporal variability (e.g., Indian summer monsoon, dipole, etc.) of the resultant flux fields.

Surface flux fields are usually developed from atmospheric general circulation models (GCM) such as the National Centers for Environmental Prediction (NCEP) reanalyses (Kalnay et al. 1996; Kanamitsu et al. 2002) and the European Centre for Medium-Range Weather Forecasting

(ECMWF) reanalyses (Gibson et al. 1997). The GCM products represent the integration of atmospheric observational networks with GCMs over an extended retrospective period using a consistent data assimilation and model structure. When compared with in-situ products, advantages of these fields are better temporal resolution and the addition of upper-air fields. The fallbacks with using GCM fluxes are large biases in heat fluxes (Smith et al. 2001; Bony et al. 1997) and a poor handling of the wind field in equatorial regions (Putman et al. 2000).

The objective method employed during this study builds upon previous versions of the FSU Winds climatology (Bourassa et al. 2005). The technique is used to create monthly fields of surface fluxes (latent and sensible heat and wind stress) for the Indian Ocean region (29.5°E, 29.5°S and 120.5°E, 29.5°N, Fig. 1). The spatial and temporal grid spacings are 1° and one month respectively. The current flux product is a vast improvement over our previous version (Jones et al. 1995), a product with a 2° grid spacing.

Previous studies using in-situ observations (Josey et al. 1999; Yu et al. 2004) were created with various objective methods and parameterizations. Josey et al. (1999) attempted to globally scale their 1° monthly flux product using closure of the heat budget. They found that regional adjustments must be made to the fluxes to obtain closure. The flux product development of Yu et al. (2004) combined satellite retrieval, output of numerical weather prediction models, and ship observations to produce daily fields with a spatial resolution of 1°. We will show that our product clarifies spatial and temporal variability influenced by large scale phenomena such as the annual monsoon reversal and ENSO.

In the tropical Indian Ocean a pattern of internal variability exists independently of ENSO. The spatial/temporal pattern is termed the Indian Ocean Dipole (IOD) mode. First discovered by Saji

---

*Corresponding Author address:* Robert F. Banks  
Center for Ocean-Atmospheric Prediction Studies,  
Florida State University, 2035 E. Dirac Dr., Suite  
200 Johnson Bldg., Tallahassee, FL 32306-  
3041. Email: banks@coaps.fsu.edu Phone: (850)  
459-7467

et al. (1999), its distinguishing characteristics are anomalously low sea surface temperatures off Sumatra and high sea surface temperatures in the western Indian Ocean. The spatial anomalies are coupled with anomalous precipitation and wind patterns through ocean-atmospheric dynamics (Ashok et al. 2004). The research contained in this paper analyzes an objectively determined series of monthly flux fields for a 22-year period (January 1978-December 2003). EOF analyses indicate variability on temporal scales from semi-annual to biennial. We exhibit EOF3 as the dipole mode of surface turbulent fluxes. Time evolution and correlation of surface fluxes with the IOD are also established.

The data and quality control used for this study are described in Section 2. In Section 3, we explain the objective analysis technique employed to grid the in-situ ship and buoy observations. Also Section 3, the bulk formulae used in calculating the surface fluxes are presented. Results are discussed in Section 4. Finally, we summarize our results and discuss remaining issues in Section 5.

## 2. DATA AND QUALITY CONTROL

### *a. Data sets*

The in-situ ship and buoy observations used in creating the gridded fields are obtained from two sources. Observations from 1982 through 1997 are extracted from the International Comprehensive Ocean-Atmosphere Data Set (ICOADS; Worley et al. 2005). The ICOADS Data Set encompasses historical marine data for the extended period of 1784 through 1997. Data from 1998 through 2003 are extracted from the National Climatic Data Center (NCDC) Marine Surface Observations (TD-1129; NCDC 2003). TD-1129 contains all available marine reports from 1982 to the present; however, some are duplicated.

Monthly means of air temperature ( $A_T$ ), specific humidity ( $q$ ), scalar wind speed ( $w$ ), and pseudostress components ( $\psi_x$  and  $\psi_y$ ) are developed from the two data sets (see Section 2.2 for quality control). The monthly means are determined for  $1^\circ \times 1^\circ$  cells containing at least 30% surface water based on topography with 5 minute resolution. The Indian Ocean study region is  $29.5^\circ\text{S}$  to  $29.5^\circ\text{N}$ ,  $29.5^\circ\text{E}$  to  $120.5^\circ\text{E}$  for the period beginning January 1982 through December 2003. The pseudostress components are the product of the wind component ( $u$ ,  $v$ ) and the scalar wind ( $w$ ).

Anemometer observations of wind speed from ships are assumed to correspond to a reference

height of 20m. These wind speed observations are height adjusted to the WMO standard height of 10m through the use of a flux model (Bourassa et al. 1999). An adjustment (Lindau 1995) is also applied to visually estimated (Beaufort) winds to correct for wind speed biases and adjust to a 10m reference height. Moored buoy measurement heights are known and then height adjusted to 10m. The wind speed observations from drifting buoys are assumed a calibration of 10m prior to our extraction.

Sea surface temperature (SST) data for the period of study (1982-2003) are obtained from a third source. Monthly linear optimum interpolation (OI) analyses are extracted from the National Meteorological Center (NMC) Climate Diagnostics Center (CDC) global product (Reynolds et al. 1998). The Reynolds et al. (2002) analysis uses in-situ and satellite SST's plus SST's derived from sea-ice concentration. The product results in higher accuracy in areas of sparse in-situ data due to the addition of satellite data.

### *b. Data quality control*

In-situ data sets have a small fraction of large errors that can be caused by incorrect records of ship locations, instrument malfunctions and misuse, etc. (Bourassa 2005). The ICOADS Data Set includes a detailed quality control procedure such as identifying the type of observing platform associated with each observation (where available), comparing individual observations to climatology, and eliminating duplicate reports (Worley et al. 2005). The TD-1129 product (NCDC 2003) applies similar checks except for checking for duplicate reports. Three additional quality control procedures are applied to the data at the Center for Ocean-Atmospheric Prediction Studies (COAPS) before using the objective analysis method. The first quality control procedure is applied to the original observations while the latter two are applied to monthly mean gridded observations.

First, the individual observations are compared to climatological values. Gross outliers are removed by this check. A monthly mean and standard deviation is computed using the daSilva climatology (daSilva et al. 1994). We accept all data within 3.5 standard deviations from the monthly mean. A minimum standard deviation accounts for limited variability of the DaSilva climatology in some parts of the globe (Bourassa et al. 2005).

Prior to executing the final two quality control procedures, monthly mean fields are generated from the in situ observations binned on a 1°x1° grid. Observations are recorded at varying time intervals and spatial distributions depending on the platform. Moored buoy reports are typically collected every hour at the same location while drifting buoys generally collect data every ten hours at different locations. Ship reports are collected every six hours at different locations. Due to the sampling characteristics of the observing platform, as well as a lack of independence of hourly data, moored buoy reports are daily averaged prior to the calculation of a monthly mean.

“Auto-flag” is a new objective quality control process developed at COAPS and is the second step in quality assuring the data. Using a ranking system of flags to diagnose suspect data, this process eliminates grid points that differ too much from adjacent grid points. A datum is removed based on the number of flags received for excessive differences from neighboring values (see Appendix A for more details). The auto-flag check greatly reduces the amount of time necessary for the next procedure.

The final quality control implements a tool developed to subjectively review the monthly mean binned observations. Using this utility, an analyst visually inspects the data and removes questionable observations that were not removed by the previous two routines (Appendix A). The procedure can be time intensive for the analyst when there are a lot of data to remove. As result of the auto-flag system’s creation, the processing time has decreased by nearly a factor of ten. The final two procedures greatly reduce the amount of smoothing required by the objective analysis method.

### 3. OBJECTIVE ANALYSIS METHOD

#### a. Variational method

A variational method is exploited to objectively grid in-situ (ship and buoy) observations in the Indian Ocean. The objective fields are produced on a 1° grid for the region 29.5°N to 29.5°S, 29.5°E to 120°E. The objective method is employed iteratively with subjective editing in the data, to remove the relatively large inconsistencies between the input data and the solution fields. Errors caused by incorrect ship position and poor sampling are usually the culprit for such inconsistencies. Variational analysis methods

allow information in various forms to be combined by minimizing a lack of fit to a set of constraints (Jones et al. 1995). A direct minimization scheme (Shanno and Phua 1980) employs a cost function based on several weighted constraints.

The cost function ( $f$ ) for a vector variable

(e.g., wind stress) is

$$f = \sum_{i,j} \beta_{\tau_{oi}} \sigma_{\tau_{oi}}^{-2} [(\tau_x - \tau_{x_{oi}})^2 - (\tau_y - \tau_{y_{oi}})^2] + \beta_{\tau_{o2}} \sigma_{\tau_{o2}}^{-2} [(\tau_x - \tau_{x_{o2}})^2 - (\tau_y - \tau_{y_{o2}})^2] + \beta_g L^4 [\nabla^2 (\tau_x - \tau_{x_{bg}})^2] + \beta_g L^4 [\nabla^2 (\tau_y - \tau_{y_{bg}})^2] + \beta_h L^2 [\hat{k} \cdot \nabla \times (\bar{\tau} - \bar{\tau}_{bg})^2]$$

where the  $\beta$ 's are weights, the  $i, j$  subscripts for geographical position have been dropped (the  $\beta$ 's and  $L$  are the only terms that do not vary

spatially), the unsubscripted wind stress ( $\tau_x, \tau_y$ ) is the solution field, the 'o' subscript indicates observations ('o1' for ships and 'o2' for moored buoys applied independently), the subscript 'bg' indicates the background field,  $\sigma$  is an estimate of the uncertainty in the observed mean, and  $L$  is a grid-spacing dependent length scale that make the weights approximately independent of grid spacing.

Three types of constraints are applied to each vector variable. The constraints are misfits to each type of observation, a Laplacian smoothing term, and a misfit of the curl. The last two constraints are applied to differences between the solution field and a background field. Scalar variables are only subject to the first two constraints. The misfit of the curl is applicable to all vector variables. The constraints used in the variational method maximize the similarity to observations as well as minimize non-geophysical features in the spatial derivatives. The method accomplishes these goals with the minimum amount of smoothing necessary. Prior to minimization of the cost function, the weights ( $\beta$ ) are determined using cross-validation (Pegion et al. 2000). For a more detailed description of the variational method, including an explanation of the weighted constraints and the background field construction, see Appendix B.

#### b. Flux calculations

In-situ measurements of surface fluxes are infrequently measured over the global oceans.

Therefore, zonal ( $\tau_x$ ) and meridional ( $\tau_y$ ) wind stress, sensible heat flux ( $H$ ), and latent heat flux ( $E$ ) are calculated using bulk aerodynamic flux algorithms (Bourassa et al. 2005). The monthly mean fluxes are estimated using monthly mean values of temperatures, humidity, and winds.

$$\tau_x = \rho_a C_D \Psi_x,$$

$$\tau_y = \rho_a C_D \Psi_y,$$

$$H = \rho_a c_p C_H (SST - AT) w,$$

$$E = \rho_a L_v C_E (q_{sfc} - q) w,$$

where  $\rho_a$  is the density of moist air,  $c_p$  is the specific heat of air at constant pressure, and  $L_v$  is the latent heat of vaporization. The bulk transfer coefficients ( $C_D$ ,  $C_H$ , and  $C_E$ ) are determined from the Bourassa et al. (2005) flux model. The minimization of the cost function produces monthly maps of the surface variables (e.g., temperature, humidity, and psuedostress) as well as surface turbulent fluxes.

#### 4. RESULTS

The objective analysis method (Section 3) is used to create monthly mean fields of the surface input variables and surface turbulent fluxes for the 22-year period. The results of this study will focus on the surface fluxes.

##### a. Climatology

In an approach to isolate the annual cycle, monthly surface flux fields are averaged e.g., (all January, all February, etc.) over the period of 22 years. The resulting product is a monthly climatology of wind stress, latent heat flux, and sensible heat flux. Variability of surface fluxes is predominantly influenced by the annual monsoon reversal in the north Indian Ocean. Areas with noticeable annual changes in wind stress are the Red Sea, Gulf of Aden, Persian Gulf, and Gulf of Oman. During the Indian summer monsoon, the wind stress values are maximum in the western Arabian Sea and the southeast trade wind belt (Fig. 2a). The largest value of approximately  $0.30\text{Nm}^{-2}$  occurs off the coast of Somalia in

association with the Findlater Jet. In the Gulf of Aden during the Indian summer monsoon, the wind stress magnitude is more than 50% less than the wind stress off the coast of Somalia. The wind stress magnitude in the Gulf of Aden is only  $0.06\text{Nm}^{-2}$  in August. The difference in magnitudes between the Gulf of Aden and Arabian Sea is only observed in the Indian summer monsoon when the winds are southwesterly. Topographic effects south of the Gulf of Aden most likely reduce the wind speed thus reducing the wind stress. The wind stress reverses direction to northeasterly during the Asian winter monsoon with maximum values in the South China Sea (Fig. 2b). The magnitude of wind stress due to the Asian monsoon is not as strong in comparison to the Indian summer monsoon. The largest magnitude during the Asian monsoon is approximately  $0.17\text{Nm}^{-2}$  northeast of Vietnam. In the same season as the Asian winter monsoon, another high pressure builds off of Australia increasing wind stress values in the southeast trade wind region. The Australian summer monsoon enhances wind stress in the southeast trades and a strong southerly wind stress develops along the west coast of Australia with a maximum of  $0.15\text{Nm}^{-2}$ . An annual cycle of wind stress is also observed in the Red Sea. During the Indian summer monsoon (Fig. 2a), the wind stress in the Red Sea is northwest off the coast of Egypt with a typical magnitude of  $0.1\text{Nm}^{-2}$ . When the Asian winter monsoon builds in (Fig. 2b), the northwesterly wind stress ( $0.1\text{Nm}^{-2}$ ) off Egypt converges with southeasterly stress ( $0.06\text{Nm}^{-2}$ ) coming from a small strait that separates the Red Sea from the Gulf of Aden. Another wind stress circulation with a pronounced annual cycle occurs between the Persian Gulf and Gulf of Oman. During the Asian monsoon, the wind stresses in both basins are northwesterly with magnitudes of near  $0.06\text{Nm}^{-2}$ . When the Indian summer monsoon is active (Fig. 2a), the wind stress converges between the two basins near the Strait of Hormuz. Wind stress values are typically small ( $0.05\text{Nm}^{-2}$ ) in this region year-round.

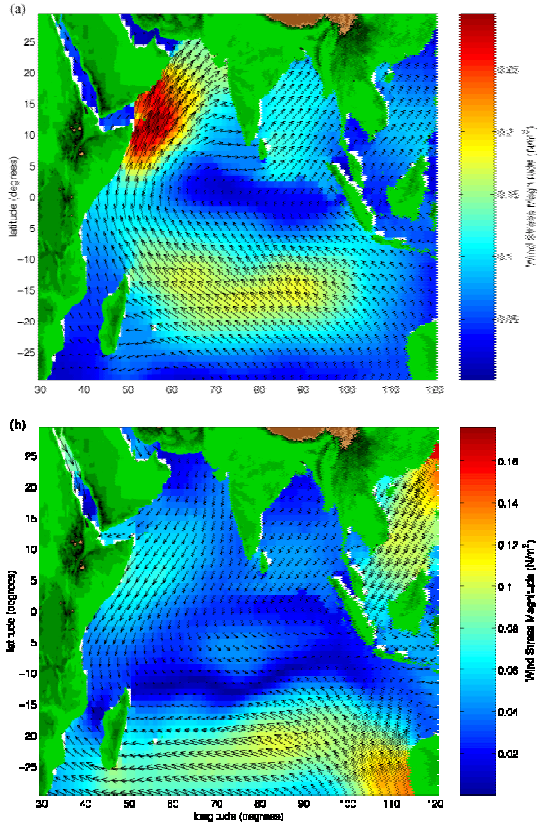


FIG. 2. Climatology of the wind stress created from 22 years of monthly objective analysis results. (a) August and (b) February are shown as representative months of peak summer and winter monsoon periods respectively. Units are  $\text{Nm}^{-2}$ .

Latent heat fluxes in the boreal summer months are sustained by the strong (Indian) monsoon winds. Maximum values of generally  $140\text{Wm}^{-2}$  to  $180\text{Wm}^{-2}$  are observed in the southeasterly trades, northeast of Madagascar, west of Sumatra, and in the Arabian Sea east of Somalia (Fig. 3a). In previous studies (Surgi, 1991) it has been discovered that coastal upwelling suppresses fluxes along the Somali coast due to strong along-coast winds. The strong along-coast winds decrease evaporation thus suppressing latent heat. In addition to the Somali coast we find decreased flux values east of Tanzania and along the coast of Sri Lanka. In boreal winter (Fig. 3b), maximum values are generally  $150\text{Wm}^{-2}$  to  $170\text{Wm}^{-2}$  and they occur in the South China Sea, off the west coast of Australia, the Arabian Sea, and in the north Red Sea.

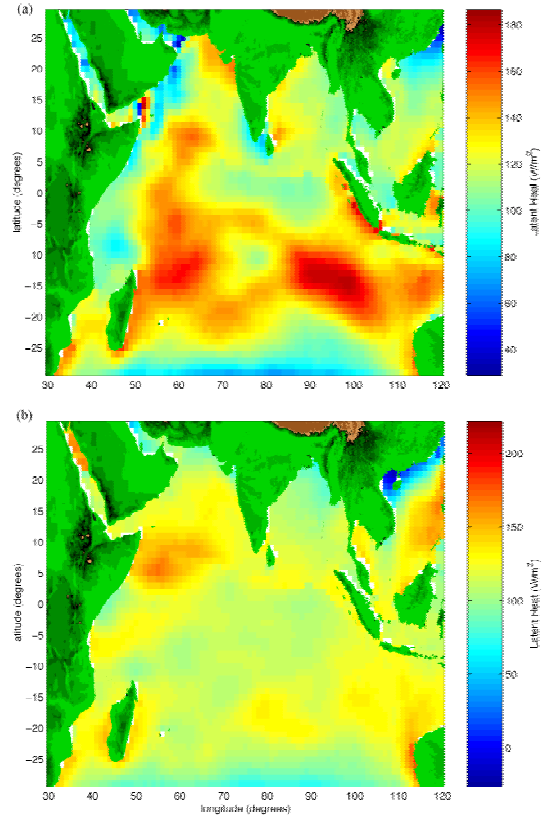


FIG. 3. Climatology of the latent heat flux obtained as in Figure 2. (a) August and (b) February are representative months of the peak summer and winter monsoon periods respectively. Units are  $\text{Wm}^{-2}$ .

Sensible heat flux in the boreal summer is maximum west of Australia and in the southeast trades, off the east coast of South Africa, south of Madagascar, and along the west coast of Sumatra (Fig. 4a). Generally these maximum values range from  $30\text{Wm}^{-2}$  to  $45\text{Wm}^{-2}$ . The large values of sensible heat flux are attributed to large air-sea temperature differences and strong winds associated with the Indian summer monsoon. Values are generally  $5\text{Wm}^{-2}$  to  $15\text{Wm}^{-2}$  everywhere else in the basin with the lower values occurring in regions with coastal upwelling. During the Asian winter monsoon (Fig. 4b), sensible heat flux values are maximum in the South China Sea and off the west coast of Australia. Maximum values generally range from  $40\text{Wm}^{-2}$  near Australia to  $50\text{Wm}^{-2}$  in the South China Sea. Air-sea temperature differences are small elsewhere

in the Indian Ocean resulting in small flux values of  $\pm 10 \text{ Wm}^{-2}$ .

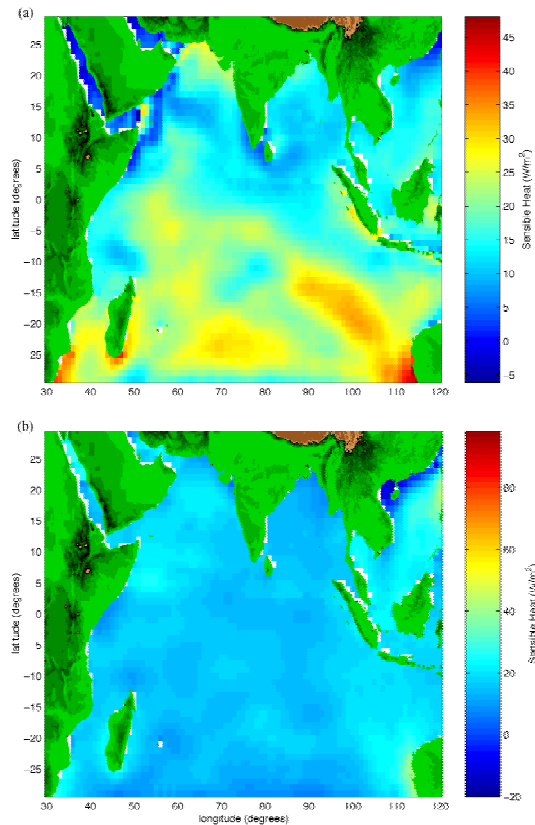


FIG. 4. Climatology of the sensible heat flux obtained as in Figure 2. (a) August and (b) February are representative months of the peak summer and winter monsoon periods respectively. Units are  $\text{Wm}^{-2}$ .

## 5. CONCLUSIONS

In this study, we presented a new methodology for objectively gridding surface turbulent fluxes over the Indian Ocean. Using our improved flux fields we exhibited spatial and temporal variability such as the Indian Ocean Dipole (IOD) mode and the annual monsoon reversal. Further research is ongoing and will be presented at the AMS meeting.

**Acknowledgements.** The author would like to acknowledge Prof. James J. O'Brien and Prof. Carol Anne Clayson for acting as committee members. A special thank you to Prof. Mark A. Bourassa for being an excellent advisor. Also, thank you to Dmitry Dukhovskoy for help with graphics and Melissa Griffin for helpful review and

comments. Thanks to Jeremy Rolph for his hardwork and help in developing the flux fields. This study was partly funded by NOAA OCO and the NSF with COAPS base funding from NOAA CDEP.

## References

- Ashok K., Z. Guan, N.H. Saji, and T. Yamagata. 2004: **On the individual and combined influences of the ENSO and the Indian Ocean Dipole on the Indian Summer Monsoon.** *Journal of Climate*: 17, pp. 3141-3154.
- Bony S., Y. Sud, K. M. Lau, J. Susskind and S. Saha. 1997: **Comparison and Satellite Assessment of NASA/DAO and NCEP-NCAR Reanalyses over Tropical Ocean: Atmospheric Hydrology and Radiation.** *Journal of Climate*: Vol. 10, No. 6, pp. 1441-1462.
- Bourassa M.A., R. Romero, S.R. Smith and J.J. O'Brien. 2005: **A New FSU Winds Climatology.** *Journal of Climate*: Vol. 18, No. 17, pp. 3686-3698.
- Bourassa M.A., D.G. Vincent and W.L. Wood. 1999: **A Flux Parameterization Including the Effects of Capillary Waves and Sea State.** *Journal of the Atmospheric Sciences*: Vol. 56, No. 9, pp. 1123-1139.
- da Silva, A., A. C. Young, and S. Levitus. 1994: **Algorithms and Procedures. Vol. 1. Atlas of Surface Marine Data 1994:** NOAA Atlas NESDIS 6, 83 pp.
- Gibson J., S. Kallberg, S. Uppala, A. Nomura, A. Hernandez, and E. Serrano. 1997: **ERA description. ECMWF Reanalysis Project Report Series 1, Tech. Rep. 1. ECMWF:** Shinfield Park, Reading, United Kingdom, 72 pp.
- Jones, C. S., D. M. Legler and J. J. O'Brien. 1995: **Variability of surface fluxes over the Indian Ocean; 1960-1989.** *Global Atmosphere-Ocean System*: 3, pp. 249-272.
- Josey, S. A., E. C. Kent and P. K. Taylor. 1999: **New insights into the ocean heat budget closure problem from analysis of the SOC air-sea flux climatology.** *Journal of Climate*: 12(9), pp. 2856 - 2880.

- Kalnay E., M. Kanamitsu, R. Kistler, W. Collins, D. Deaven, L. Gandin, M. Iredell, S. Saha, G. White, J. Woollen, Y. Zhu, A. Leetmaa, B. Reynolds, M. Chelliah, W. Ebisuzaki, W. Higgins, J. Janowiak, K.C. Mo, C. Ropelewski, J. Wang, Roy Jenne and Dennis Joseph. 1996: **The NCEP/NCAR 40-Year Reanalysis Project**. *Bulletin of the American Meteorological Society*: Vol. 77, No. 3, pp. 437–471.
- Kanamitsu M., W. Ebisuzaki, J. Woollen, S.K. Yang, J. J. Hnilo, M. Fiorino and G.L. Potter. 2002: **NCEP–DOE AMIP-II Reanalysis (R-2)**. *Bulletin of the American Meteorological Society*: Vol. 83, No. 11, pp. 1631–1643.
- Lindau, R. 1995a: **A new Beaufort equivalent scale**. *COADS Winds Workshop*: 1 May - 2 June 1994, Kiel, Germany, (Kiel: Institut fur Meereskunde/Christian-Albrechts-Universitat), pp. 232-252.
- NCDC. 2003: **Data documentation for data set 1129**. *National Climatic Data Center*. 151 Patton Ave., Asheville, NC 28801-5001 USA
- Pegion, P. J., M. A. Bourassa, D. M. Legler, and J. J. O'Brien. 2000: **Objectively derived daily "winds" from satellite scatterometer data**. *Mon. Wea. Rev.*: **128**, pp. 3150–3168.
- Putman W.M., D.M. Legler and J.J. O'Brien. 2000: **Interannual Variability of Synthesized FSU and NCEP-NCAR Reanalysis Pseudostress Products over the Pacific Ocean**. *Journal of Climate*: Vol. 13, No. 16, pp. 3003–3016.
- Reynolds, R. W., N. A. Rayner, T. M. Smith, D. C. Stokes and W. Wang. 2002: **An improved in situ and satellite SST analysis for climate**. *Journal of Climate*: 15, pp. 1609-1625.
- Saji, N.H., B.N. Goswami, P.N. Vinayachandran, and T. Yamagata. 1999: **A dipole mode in the tropical Indian Ocean**. *Nature*: 401, pp. 360-363.
- Shanno, D. F., and K. H. Phua. 1980: **Remark on Algorithm 500—A variable method subroutine for unconstrained nonlinear minimization**. *ACM Trans. Math. Software*: **6**, pp. 618–622.
- Smith, S. R., D. M. Legler, and K. V. Verzone. 2001: **Quantifying uncertainties in NCEP reanalyses using high quality research vessel observations**. *Journal of Climate*. 14, pp. 4062-4072.
- Smith, S.L., K. Banse, J.K. Cochran, L.A. Codispoti, H.W. Ducklow, M.E. Luther, D.B. Olson, W.T. Peterson, W.L. Prell, N. Surgi, J.C. Swallow, and K. Wishner. 1991: **U.S. JGOFS: Arabian Sea Process Study**. *U.S. JGOFS Planning Report Number 13*: Woods Hole Oceanographic Institution, 164 pp.
- Worley, S. J., S. D. Woodruff, R. W. Reynolds, S. J. Lubker, and N. Lott. 2005: **ICOADS Release 2.1 data and products**. *Int. J. Climatol.*: 25, pp. 823-842.
- Yu, L., R. A. Weller, and B. Sun. 2004: **Mean and variability of the WHOI daily latent and sensible heat fluxes at in situ flux measurement sites in the Atlantic Ocean**. *Journal of Climate*: 17, pp. 2096-2118.